

## Study of E2 transition probabilities and g-factors of even-even Curium isotopes

<sup>1</sup>Saiqa Sadiq, <sup>2</sup>Rani Devi and <sup>3</sup>S.K. Khosa

*Department of Physics and Electronics,  
University of Jammu, Jammu-180006, INDIA  
saiqahep@gmail.com*

### ABSTRACT

The existence of super heavy elements is one of the major issues in nuclear physics. Many experimental and theoretical efforts have been made to study the super heavy elements during last decades. In order to achieve reliable predictions in the super heavy mass region, a good understanding of the properties of heavy mass nuclei is essential. In the present work, the B(E2) transition probabilities and g-factors of even-even Curium (Cm) isotopes have been studied by using projected shell model approach, which is a bridge connecting the shell model and mean-field approaches. The E2 transition probabilities and g-factors have been calculated by using the many body wave functions that reproduce the ground state bands of Cm isotopes. The calculated B(E2) values reproduces the available experimental data. The predicted values of B(E2)s, show an increasing trend with spin and the predicted values of g-factors show a slight variation at higher spins. The energy states of these nuclei at lower spin arise from almost pure quasiparticle configuration in which all the nucleons are paired. Therefore, g-factors of these nuclei with spin are not showing much variation. The predicted values of E2 transition probabilities are useful in understanding the properties of nuclear excitations and electromagnetic quantities of Cm isotopes needs experimental confirmation.

### 1 Introduction

Much of current research in nuclear physics relates to the study of nuclei under extreme conditions such as high spin and excitation energies. Nuclei may also have extreme shapes or extreme neutron to proton ratios. A heavy nucleus contains hundreds of nucleons. Actinide nuclei are not only among the heaviest elements for which quantitative spectroscopic information can be obtained, but are also among the most deformed and hence the most collective nuclei available for experimental investigation [1-6]. The actinides furnish a testing ground for theoretical models. In this regard Curium nuclei constitute an important mass chain for making nuclear structure study and testing of some established calculational frameworks. In the past, Ahmed et al [7] have observed the existence of the ground state rotational bands with identical transition energies up to spin  $I=8\hbar$  in  $^{244}\text{Cm}$  and  $^{246}\text{Cm}$  and have found that the importance of these bands is that the single particle states are well characterized at normal deformed and hence there is better chance of understanding the underlying physics in these identical bands

The experimental data reveal that the Curium isotopes show well-deformed band spectra. At low spins, near the ground state they exhibit very similar collective behavior with regular rotational level sequence. This tells us that near the ground state these nuclei behave like rigid rotors. They show strong collectivity, diluting any individual role of single particles. Therefore, not much information can be extracted from these low spin rotor states. More useful information may be



obtained through the study of high spin states with quasi-particle (qp) excitation. Apart from this, a theoretical study of high spin states of all the Curium isotopes can provide very important understanding of the nuclear structure properties of these nuclei. Therefore, in the present work an attempt has been made to study the nuclear structure properties of Curium isotopes in the framework of Projected Shell Model (PSM) [8] by employing quadrupole-quadrupole plus monopole and quadrupole-pairing force in the Hamiltonian. PSM is based on the spherical shell model concept. It differs from the conventional shell model in that the PSM uses the angular momentum projected states as the basis for the diagonalization of the shell model Hamiltonian.

## 2 Calculational Framework

In this section, a brief presentation of the PSM approach is given and the detailed description of PSM can be found in the review article [9]. The PSM is based on the spherical shell model concept. It differs from the conventional shell model in that the PSM uses the angular momentum projected states as the basis for the diagonalization of the shell model Hamiltonian.

The angular momentum projected wave function for the PSM is given by

$$|IM\rangle = \sum_k f_k \hat{P}_{MK}^I |\varphi_k\rangle \quad (1)$$

where  $\hat{P}_{MK}^I$  is the angular momentum projection operator and the coefficients  $f_k$  are the weights of the basis state  $k$  which are determined by the diagonalization of the shell model Hamiltonian in the space spanned by the projected basis states given above.

The projection of an intrinsic state  $|\varphi_k\rangle$  onto a good angular momentum generates the rotational energy

$$E_k(I) = \frac{\langle \varphi_k | \hat{H} \hat{P}_{KK}^I | \varphi_k \rangle}{\langle \varphi_k | \hat{P}_{KK}^I | \varphi_k \rangle} = \frac{H_{kk}^I}{N_{kk}^I} \quad (2)$$

The energies of each band,  $E_k(I)$ , are given by the diagonal elements of  $H_{kk}/N_{kk}$ . A diagram in which  $E_k(I)$  for various bands is plotted against the spin  $I$  is referred as band diagram [8], which contains incredibly rich information.

In the numerical calculations, we have used the standard quadrupole-quadrupole plus (monopole and quadrupole) pairing force, i.e.

$$\hat{H} = H_0 - \frac{1}{2}\chi \sum_\mu \hat{Q}_\mu^\dagger \hat{Q}_\mu - G_M \hat{P}^\dagger \hat{P} - G_Q \sum_\mu \hat{P}_\mu^\dagger \hat{P}_\mu \quad (3)$$

The first term  $H_0$  is the spherical single-particle Hamiltonian. The strength of the quadrupole force  $\chi$  is adjusted such that the known quadrupole deformation parameter  $\varepsilon_2$  is obtained by the usual Hartree+BCS self consistent procedure. The monopole pairing force constants  $G_M$  are adjusted to give the known energy gaps. For all the calculations, the monopole pairing strengths  $G_M$  used in the calculation are

$$G_M = \left[ 20.12 \mp 13.13 \frac{N-Z}{A} \right] A^{-1} \quad (4)$$



with ‘-’ for neutrons and ‘+’ for protons. These strengths are taken from [9]. The quadrupole pairing strength strength  $G_Q$  is assumed to be proportional to  $G_M$ .

Electromagnetic transitions can give important information on the nuclear structure and provide a stringent test of a particular model. In the present work, we have calculated the electromagnetic properties using PSM approach. The matrix elements of a quadrupole operator  $\hat{Q}_{LM}$  with respect to the (final) shell-model wave functions can be evaluated by using the formula

$$\langle \Psi_{I_f M_f} | \hat{Q}_{LM} | \Psi_{I_i M_i} \rangle = (I_i M_i, LM | I_f M_f) \langle \Psi_{I_f} \| \hat{Q}_L \| \Psi_{I_i} \rangle \quad (5)$$

The reduced transition probabilities  $B(EL)$  from the initial state  $I_i$  to the  $I_f$  are given by [10]

$$B(EL, I_i \rightarrow I_f) = \frac{e^2}{(2I_i + 1)} \left| \langle \Psi_{I_f} \| \hat{Q}_L \| \Psi_{I_i} \rangle \right|^2 \quad (6)$$

The gyro magnetic factors ( $g$ -factors) are defined by [10]

$$g(I) = \frac{\mu(I)}{\mu_N I} = g_\pi(I) + g_\nu(I), \quad (7)$$

with  $g_\tau(I)$ ,  $\tau = \pi, \nu$  given by

$$g_\tau(I) = \frac{1}{\mu_N [I(I+1)]^{1/2}} [g_l^\tau \langle \psi_I \| \hat{J}^\tau \| \psi_I \rangle + (g_s^\tau - g_l^\tau) \langle \psi_I \| \hat{S}^\tau \| \psi_I \rangle] \quad (8)$$

and  $\mu(I)$  is the magnetic moment of a state  $|\psi_I\rangle$ .

In our calculations, the following standard values of  $g_l$  and  $g_s$  have been taken

$$g_l^\pi = 1, g_l^\nu = 0, \\ g_s^\pi = 5.5860.75 \text{ and } g_s^\nu = -3.8260.75,$$

where  $g_s^\pi$  and  $g_s^\nu$  are damped by a usual 0.75 factor from the free-nucleon values to account for the core-polarization and meson-exchange current corrections [11-13].

The present calculations are performed by considering three major shells  $N = 4, 5, 6$ (5,6,7) for protons(neutrons) for the valence single-particle space. We emphasize that, unlike cranking mean-field approaches, the deformation parameters used as an input to the PSM calculations need not correspond exactly to the true nuclear deformation. This is because of the shell model nature of the PSM: the deformed single-particle states serve solely as a way to truncate the shell model basis. All observable properties in the PSM calculations are determined by the many-body wave functions obtained by diagonalizing the shell model Hamiltonian. The chosen energy window around the Fermi surface gives rise to a basis space,  $|\varphi_k\rangle$  in equation (1), of the order of 67. The basis states are projected to good angular momentum states, and the projected basis is then used to diagonalize the shell model Hamiltonian. The diagonalization gives rise to the energy spectrum, and electromagnetic quantities are calculated by using the resulting wave functions.

### 3 Results and Discussion

#### 3.1 Yrast Spectra

Figure1, presents the comparison of theoretical yrast spectra with experimental data for  $^{242-248}\text{Cm}$ . The experimental data is taken from refs. [14-17]. The input deformation parameters taken for the calculation of these nuclei are listed in table 1. The quadrupole deformation parameter was



varied around the experimental values[18] to produce  $E_2^+$ energy values. The quadrupole deformation parameters were adjusted so that the energy gaps between the  $E_2^+$  and the ground state for the  $^{242-248}\text{Cm}$  are reproduced. The theoretical spectrum has been obtained for all the four isotopes up to spin 30 $\hbar$  whereas experimental level schemes of positive-parity yrast bands for  $^{242-248}\text{Cm}$  are available up to spins 26 $^+$ , 8 $^+$ , 26 $^+$ , and 30 $^+$ , respectively. It is seen from figure 1, that the PSM calculation reproduces the available yrast energy levels up to known spins qualitatively. The maximum difference between theory and experiment for highest known spins is 0.34, 0.02, 0.57 and 1.04 (in MeV), respectively for  $^{242-248}\text{Cm}$ .

### 3.2 Electromagnetic quantities

#### 3.2.1 B(E2) transition probabilities

Table 2, presents the B(E2) values of Cm isotopes calculated by using the same deformation parameters presented in table 1. In the present calculation the effective charges of 0.55e and 1.55e have been used for neutrons and protons, respectively. The experimental data [19] is available only for  $2_1^{+-\rightarrow 0^+}$  transition for  $^{244-248}\text{Cm}$ . The available experimental data is seen to be reproduced well by the present calculation. In case of  $^{248}\text{Cm}$  the experimental data is available up to spin 24 $^+$ [20]. Experimentally, the dip in the B(E2) values of  $^{248}\text{Cm}$  is observed at spin 10 $^+$ . The calculated B(E2) values reproduce the increasing trend of the observed B(E2) values upto spin 8 $^+$ . The calculated values show a small increase with spin for higher transitions upto spin 24 $^+$ .

#### 3.2.2 g-factors

Figure 2, presents the calculated results of g-factors for  $^{242-248}\text{Cm}$ . The same wave functions have been used for the calculation of g-factors as used for calculation of B(E2) values. From the figure it is seen that the theroretical total g-factors show an increasing trend in all Cm isotopes. The total contribution of g-factors is due to gp and that may be due to alignment of protons. The increase in the g-factors at higher spin in all Cm isotopes is due to crossing of g-band by 2 qp proton bands. The experimental values of g-factors in  $^{242-248}\text{Cm}$  isotopes are not available so one cannot make any comment regarding the level of agreement.

## 4 Conclusions

The PSM calculations have been performed for the  $^{242-248}\text{Cm}$ . The calculated results reproduce the experimental data of yrast bands qualitatively. The yrast states of these nuclei at lower spins arise from almost pure zero-qp configuration whereas the higher spin states have multi-quasiparticle structure. The results presented on the B(E2) transition probability are found to show reasonably good agreement with the available experimental data for all the isotopes. The calculated values of g-factors show an increasing trend with spin in all  $^{242-248}\text{Cm}$  isotopes. The small increase reflected in the g-factor at higher spins in all these isotopes is due to crossing of g-band by 2qp proton bands. The experimental values of g-factor of these are not known, so it is not possible to make a comment regarding the level of agreement.



**Table 1** Quadrupole and hexadecapole deformation parameters used in the present calculations for  $^{242-248}\text{Cm}$  isotopes

Nucleus	$^{242}\text{Cm}$	$^{244}\text{Cm}$	$^{246}\text{Cm}$	$^{248}\text{Cm}$
$\varepsilon_2$	0.260	0.260	0.260	0.260
$\varepsilon_4$	0.010	0.018	0.033	0.040

**Table 2** Comparison of calculated (Th.) and experimental (Exp.)  $B(E2)$  reduced transition probabilities (in units of  $e^2 b^2$ ) for  $^{242-248}\text{Cm}$  isotopes. Experimental data are taken from Refs. [19,20]

Transition	$^{242}\text{Cm}$		$^{244}\text{Cm}$		$^{246}\text{Cm}$		$^{248}\text{Cm}$	
	)	Exp.	Th.	Exp.	Th.	Exp.	Th.	Exp.
$2 \rightarrow 0$	-	3.136	$2.916 \pm 0.038$	3.095	$2.988 \pm 0.038$	2.888	$2.74_{-0.003}^{+0.002}$	2.861
$4 \rightarrow 2$	-	4.490	-	4.429	-	4.131	$3.58_{-0.021}^{+0.064}$	4.091
$6 \rightarrow 4$	-	4.964	-	4.893	-	4.560	$5.07_{-0.086}^{+0.06}$	4.515
$8 \rightarrow 6$	-	5.222	-	5.143	-	4.788	$5.95_{-0.019}^{+0.021}$	4.740
$10 \rightarrow 8$	-	5.398	-	5.310	-	4.936	$3.87_{-0.037}^{+0.30}$	4.885
$12 \rightarrow 10$	-	5.533	-	5.437	-	5.046	$4.83_{-0.012}^{+0.005}$	4.992
$14 \rightarrow 12$	-	5.646	-	5.541	-	5.134	$6.21_{-0.002}^{+0.016}$	5.077
$16 \rightarrow 14$	-	5.744	-	5.632	-	5.209	$4.51_{-0.004}^{+0.007}$	5.141
$18 \rightarrow 16$	-	5.825	-	5.706	-	5.246	$4.65_{-0.037}^{+0.011}$	5.152
$20 \rightarrow 18$	-	5.867	-	5.753	-	5.242	$4.78_{-0.041}^{+0.035}$	5.243
$22 \rightarrow 20$	-	5.862	-	5.764	-	5.343	$6.27_{-0.018}^{+0.064}$	5.269
$24 \rightarrow 22$	-	5.964	-	5.853	-	5.383	$5.97_{-1.881}^{+0.78}$	5.290
$26 \rightarrow 24$	-	5.987	-	5.888	-	5.359	-	5.312
$28 \rightarrow 26$	-	5.762	-	5.734	-	5.333	-	5.288
$30 \rightarrow 28$	-	5.502	-	5.639	-	5.312	-	5.254



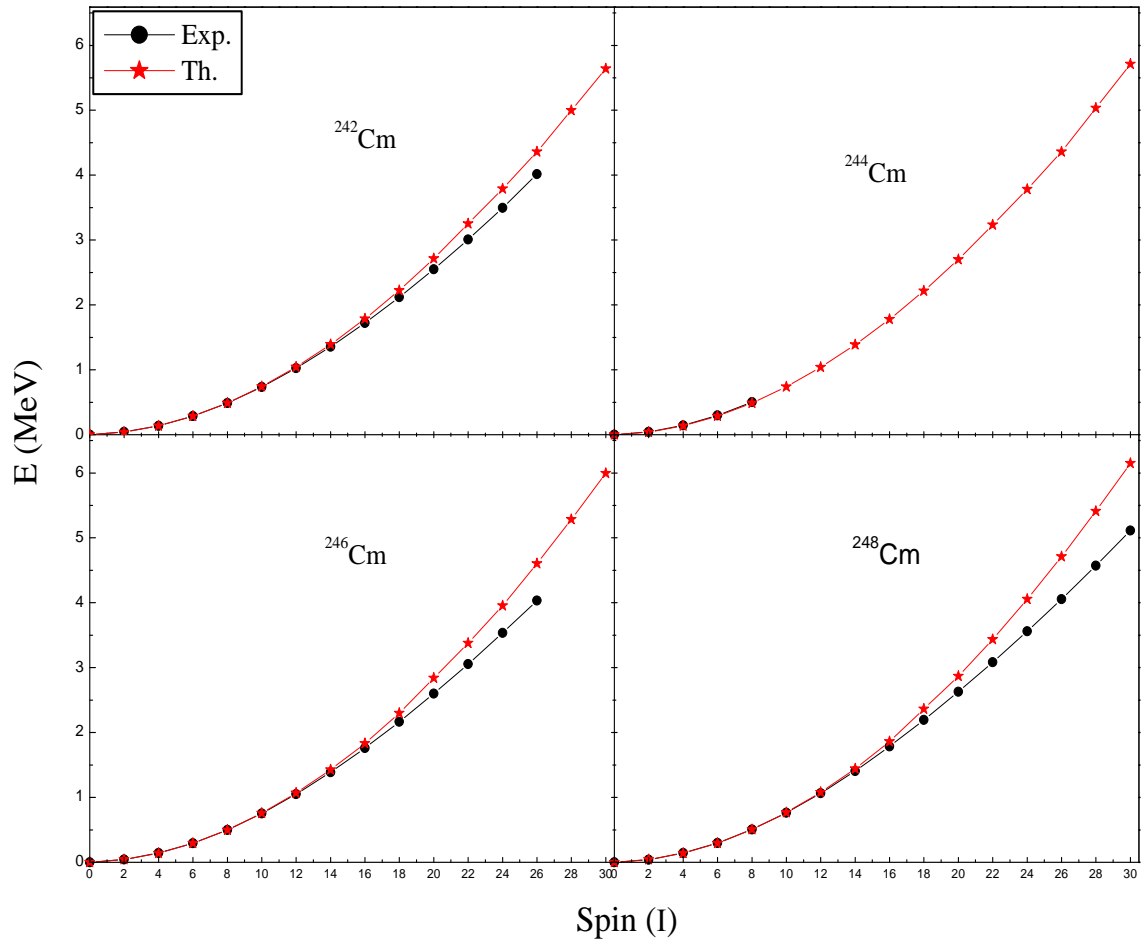


**Fig. 1** Comparison of calculated (Th.) and experimental (Exp.) positive-parity yrast bands of  $^{242-248}\text{Cm}$  isotopes. The experimental data is taken from Refs. [14-17].



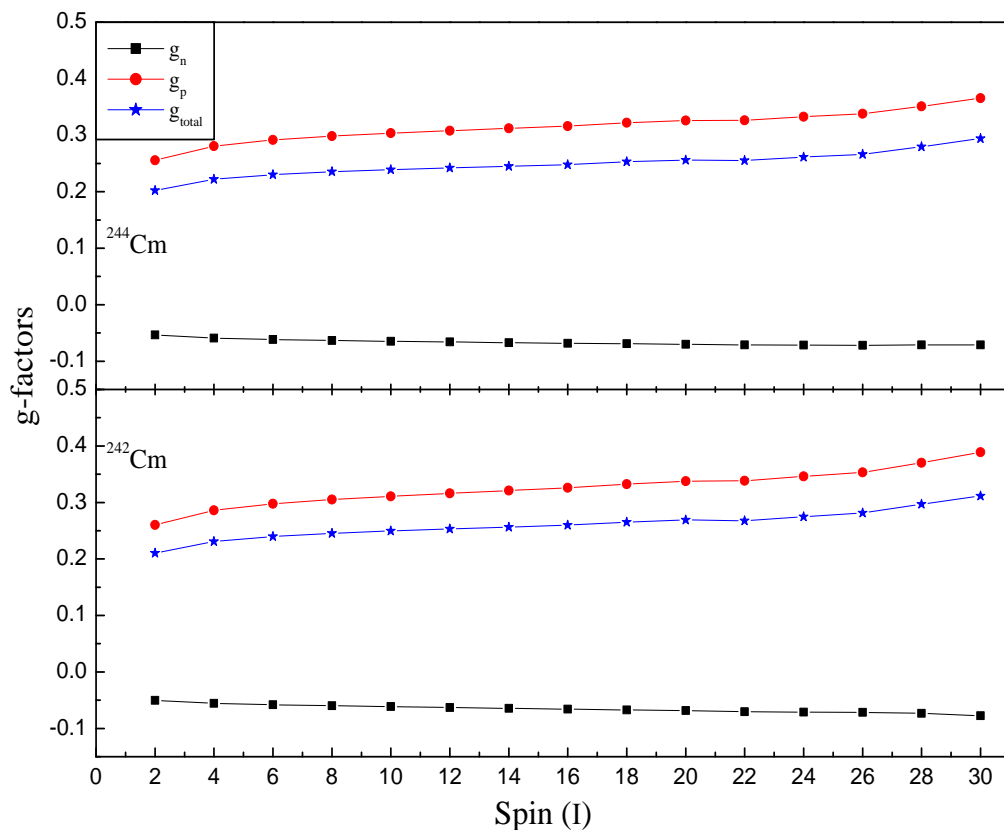


**Fig. 2** Theoretical g-factors as a function of angular momentum for  $^{242-248}\text{Cm}$  isotopes.

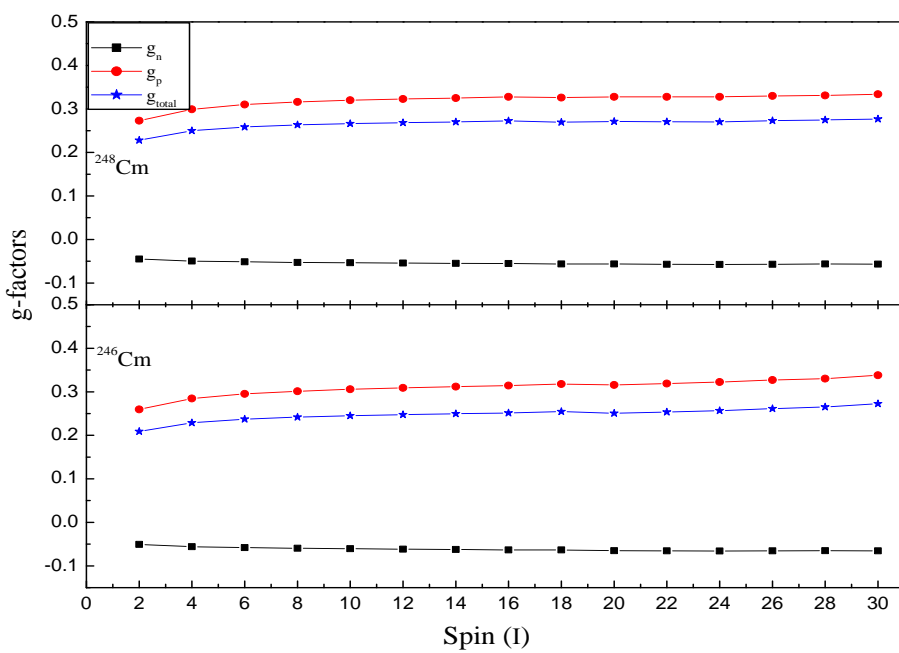


**Fig. 2 Contd.**



## References

- [1] M. Leino and F.P. Herzberger, *Ann. Rev. Nucl. Part. Sci.* **54**, 175 (2004)
- [2] R.D. Herzberg, *J. Phy. G***30**, R123 (2004)
- [3] P.T. Greenless, *Nucl. Phys. A*, **787**, 507 (2007)
- [4] R.D. Herzberg and P.T. Greenless, *Prog. Part. Nucl. Phys.* **61**, 674 (2008)
- [5] X. Wang et al., *Phys. Rev. Lett.* **102**, 122501 (2009)
- [6] A.I. Levon et al., *Phys. Rev. C***69**, 044310 (2004)
- [7] I. Ahmed, M.P Carpenter, R.R. Chasman, R.V.F Janssens and T.L Khoo, *Phys. Rev.C***44**, 1204 (1991)
- [8] K. Hara and Y. Sun, *Int. J. Mod. Phys.E***4**, 637 (1995)
- [9] D. Ram, R. Devi and S.K. Khosa, *Pramana J. Phys.* **80**, 953 (2013)
- [10] Y. Sun and J. L. Egido *Nucl. Phys A***580**, 1 (1994)
- [11] A. Bohr and B.R. Mottelson, *Nuclear StructureI*, (Benjamin, New York, Amsterdam, 1969)
- [12] B. Castel and I.S. Towner, *Modern Theories of Nuclear Moments* (Oxford-Clarendon, 1990)
- [13] J. Rikovska et al, *Phys. Rev. Lett.* **85**, 1392 (2000)
- [14] K.A. Saleem, et al., *Phys. Rev. C***70**, 024310 (2004)
- [15] Y. A. Akovali, *Nucl. Data Sheets* **99**, 197 (2003)
- [16] E. Browne, J. K. Tuli, *Nucl. Data Sheets* **112**, 1833 (2011)
- [17] M. J. Martin, *Nucl. Data Sheets* **122**, 377 (2014)
- [18] R. Bengtsson, *Suppl. J. de. Phys. C***10**, 84(1980)
- [19] S. Raman, C.W. Nestor and P. Tikkanen, *At. Data Nucl. Data Tables* **78**, 1 (2001)
- [20] T. Czosnyka, D. Cline, L. Hasselgren and C.Y. Wu, R.M. Diamond, H. Kluge, C. Roulet, E.K. Hirlet, R.W. Lougheed and C. Baktash, *Nucl. Phys. A***458**, 123 (1986)

